鉄混合原子価錯体における電荷移動相転移の動的挙動の研究

小 島 憲 道*

*小島憲道 フェロー

Study on the Dynamics of Charge Transfer Phase Transition in Iron Mixed-Valence Complexes

Norimichi KOJIMA*

In the case of mixed-valence system whose spin states are situated in the spin crossover region, conjugated phenomena coupled with spin and charge are expected. Based on this viewpoint, we have developed a ferromagnetic mixed-valence system, $A[Fe^{II}Fe^{III}(dto)_3]$ ($A = (n\text{-}C_nH_{2n+1})_4N$, spiropyran, etc,; $dto = C_2O_2S_2$), and investigated the charge transfer phase transition (CTPT) induced by the synergetic effect between spin and charge. In the cases of $(n\text{-}C_nH_{2n+1})_4N[Fe^{II}Fe^{III}(dto)_3]$ ($n = 3$ and 4), the CTPT takes place for $n = 3$ and 4. At the CTPT, the iron valence state is dynamically fluctuated with a frequency of about 0.1 MHz from the analysis of μSR. Considering that the CTPT in this system is the first order phase transition, the dynamically fluctuated valence state of iron is regarded as the fluctuation of chemical potential between the high-temperature phase and the low-temperature one. Moreover, an anomalous enhancement of dielectric constant with thermal hysteresis appears at the CTPT across the whole measuring frequency range between 1 Hz and 1 MHz, which is attributed to the valence fluctuation between the Fe^{II} and Fe^{III} sites associated with the CTPT. This anomaly becomes apparent as the frequency is lowered, which is quite similar to the dielectric relaxation in relaxor ferroelectrics.

1. INTRODUCTION

One of the most important targets in current research in the field of molecular solids is investigating the multifunctional properties coupled with transport, optical or magnetic properties. Among various multifunctional materials, in the case of mixed-valence system whose spin states are situated in the spin crossover region, it is expected that new types of conjugated phenomena coupled with spin and charge take place between different metal ions in order to minimize the Gibbs energy in the whole system. Based on this viewpoint, we have developed ferromagnetic organic-inorganic hybrid systems, $A[Fe^{II}Fe^{III}(dto)_3]$ ($A = (n\text{-}C_nH_{2n+1})_4N$, spiropyran, etc.), and discovered the charge transfer phase transition (CTPT) for $(n\text{-}C_nH_{2n+1})_4NFe^{II}Fe^{III}(dto)_3]$ ($n = 3$ and 4), where the thermally induced charge transfer between Fe^{II} and Fe^{III} occurs reversibly.[1] Moreover, at the CTPT, we found the iron valence fluctuation with a frequency of about 0.1 MHz by means of muon spin relaxation (μSR).[2] The CTPT and the ferromagnetic transition temperature in $(n\text{-}C_nH_{2n+1})_4N[Fe^{II}Fe^{III}(dto)_3]$ remarkably depend on the size of intercalated cation. Since this discovery, experimental approaches for understanding the mechanism and controlling of the CTPT for $A[M^{II}M'^{III}(dto)_3]$ have energetically been carried out.[3] In this report, the detailed dynamical behavior of the CTPT for $(n\text{-}C_3H_7)_4N[Fe^{II}Fe^{III}(dto)_3]$ by means of μSR and dielectric constant measurement techniques is presented.[4]

2. EXPERIMENTAL PROCEDURE

$(n\text{-}C_3H_7)_4N[Fe^{II}Fe^{III}(dto)_3]$ was synthesized by the following way.[1] $Fe(NO_3)_3 \cdot 10H_2O$ was treated with $K_2C_2O_2S_2$ in cold water, and the solution was filtered to remove iron sulfide. Then $BaBr_2 \cdot 2H_2O$ was added to the dark purple solution and $KBa[Fe^{III}(dto)_3] \cdot 3H_2O$ precipitated. The salt was recrystallized from water and dried. A solution of $KBa[Fe^{III}(dto)_3] \cdot 3H_2O$ in a 3 : 2 methanol/water mixture was stirred. To this was added a solution of $FeCl_2 \cdot 4H_2O$ and $(n\text{-}C_nH_{2n+1})_4NBr$ in a 3 : 2 methanol/water mixture, then a black powdered crystal precipitated. The compound $(n\text{-}C_3H_7)_4N[Fe^{II}Fe^{III}(dto)_3]$ was separated as powdered crystals by suction filtration and washed first with a 1 : 1 methanol/water mixture and then with methanol and diethyl ether. These samples were characterized by chemical analysis, powder X-ray diffraction analysis. From

2016年2月23日 受理

*豊田理化学研究所フェロー
東京大学名誉教授，理学博士
専門分野：分子集合体の物性化学，錯体化学，無機化学

the analysis of single-crystal X-ray diffraction, $(n\text{-}C_3H_7)_4N[Fe^{II}Fe^{III}(dto)_3]$ has a two-dimensional honeycomb network structure of $[Fe^{II}Fe^{III}(dto)_3]$, and the $(n\text{-}C_3H_7)_4N$ cation layer is intercalated between two adjacent $[Fe^{II}Fe^{III}(dto)_3]$ layers. Judging from the bond lengths, the Fe^{II} sites are coordinated by six oxygen atoms, while the Fe^{III} sites are coordinated by six sulfur atoms under ambient pressure.[5)]

The temperature dependence of dielectric constant was measured by two-probe method with a pellet sample. A Hewlett Packard (Keysight) 4284A Precision LCR Meter with the frequency of 1 kHz – 1 MHz and a Solartron 1260 impedance gain phase analyzer equipped with a Solartron 1269 dielectric interface with the frequency of 1 Hz – 10 MHz were employed to measure the dielectric constant. The former is suitable for high frequency range and the latter has the advantage in wide frequency region, especially in the low frequency. The measurement temperature range was between 2 and 300 K.

The μSR experiments were carried out at the RIKEN-RAL Muon Facility at the Rutherford-Appleton Laboratory in the UK and PSI Laboratory for Muon Spin Spectroscopy at the Paul Scherrer Institut in Switzerland. Polycrystalline samples of about 200 mg were wrapped in silver foils and stuck to a silver plate. We used He-flow cryostats in the temperature range between 2 and 200 K.[6)] The time dependence of the asymmetry parameter of muon-spin polarization (μSR time spectrum) was measured in zero field (ZF) and longitudinal field (LF). The asymmetry parameter is defined as $A(t) = [N_B(t) - N_F(t)]/[N_B(t) + N_F(t)]$, where $N_F(t)$ and $N_B(t)$ are total muon events of the forward and backward counters aligned in the beam line, respectively. The initial asymmetry, $A(0)$, is defined as the asymmetry at $t = 0$. The initial muon-spin polarization was parallel to the beam line and the direction of LF was parallel to the muon-spin polarization.

3. PHYSICAL PROPERTIES OF $(n\text{-}C_nH_{2n+1})_4N[Fe^{II}Fe^{III}(dto)_3]$

The most important physical properties in the series of $(n\text{-}C_nH_{2n+1})_4N[Fe^{II}Fe^{III}(dto)_3]$ are the charge transfer phase transition (CTPT) and the ferromagnetic phase transition.[1)] Figure 1 shows the schematic representation of the CTPT for $n = 3$. The magnetic susceptibilities for all the complexes obey the Curie-Weiss law, $\chi_M T = CT / (T - \theta)$ in the range of 150–300 K.[1)] In the cases of $n = 3$ and 4, reflecting the CTPT, a small hump appears in $\chi_M T$ at around 120 K and 140 K for $n = 3$ and 4, respectively.[1)] The magnetic susceptibility and electron spin resonance measurements reveal that a thermal hysteresis loop appears between 60 K and 130 K for $n = 3$, between 50 K and 145 K for $n = 4$, respectively. All the

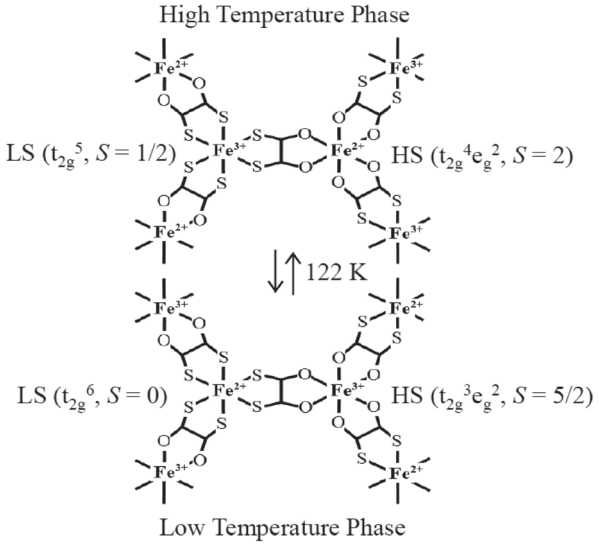

Figure 1. Schematic representation of the charge transfer phase transition (CTPT) in $(n\text{-}C_3H_7)_4N[Fe^{II}Fe^{III}(dto)_3]$.

samples of $n = 3$–6 undergo the ferromagnetic phase transition in the low temperature region. For the as-prepared sample of $(n\text{-}C_nH_{2n+1})_4N[Fe^{II}Fe^{III}(dto)_3]$, the Fe^{II} site surrounded by six oxygen atoms is situated in the high spin state (Fe^{II} ($S = 2$)), while the Fe^{III} site surrounded by six sulfur atoms is situated in the low spin state (Fe^{III} ($S = 1/2$)). The spin state with the combination between $Fe^{II}O_6$ ($S = 2$)-$Fe^{III}S_6$ ($S = 1/2$) is named as high temperature phase (HTP). In the cases of $n = 3$ and 4, judging from the heat capacity measurement, the CTPT takes place at 122.4 K and 142.8 K for $n = 3$ and 4, respectively, where an electron transfers reversibly between the t_{2g} orbitals in the Fe^{II} and Fe^{III} sites. As a result of this CTPT, the coordination environment of Fe^{II} and Fe^{III} are exchanged with each other as like $Fe^{II}S_6$ and $Fe^{III}O_6$. Additionally, the spin state of these two sites are changed as the low spin state of Fe^{II} ($S = 0$) and the high spin state of Fe^{III} ($S = 5/2$). The spin state with $Fe^{II}S_6$ ($S = 0$)-$Fe^{III}O_6$ ($S = 5/2$) is denoted as low temperature phase (LTP), which was elucidated by means of ^{57}Fe Mössbauer spectroscopy.[1, 3)] In the cases of $n = 5$ and 6, on the other hand, the CTPT does not take place in the whole measuring temperature range between 300 K and 2 K under ambient pressure. According to the temperature dependence of the field cooled magnetization (FCM), the zero-field cooled magnetization (ZFCM) and the remnant magnetization (RM) for $(n\text{-}C_nH_{2n+1})_4N[Fe^{II}Fe^{III}(dto)_3]$ ($n = 3 \sim 6$), the LTP with $Fe^{II}S_6$ ($S = 0$)-$Fe^{III}O_6$ ($S = 5/2$) configuration for $n = 3$ undergoes the ferromagnetic transition at 7 K, while the HTP with $Fe^{II}O_6$ ($S = 2$)-$Fe^{III}S_6$ ($S = 1/2$) configuration for $n = 5$ and 6 undergoes the ferromagnetic transition at 19.5 and 22 K, respectively.[1)]

4. MUON SPIN RELAXATION

Muon is a very useful elemental particle for sensing the magnitude, distribution and fluctuation of internal field. Therefore, the μSR technique has been applied to the study of magnetic phase transitions, various kinds of spin frustrations, superconducting phenomena and so forth. The asymmetry parameter is defined as $A(t) = [N_B(t) - N_F(t)]/[N_B(t) + N_F(t)]$, where $N_F(t)$ and $N_B(t)$ are total muon events of the forward and backward counters aligned in the beam line, respectively. The initial asymmetry, $A(0)$, is defined as the asymmetry at $t = 0$. To analyze the time spectra, the following function with two components was used,

$$A(t) = A_0 G_Z(\Delta, H_{LF}, t)\exp(-\lambda_0 t) + A_1 \exp(-\lambda_1 t) \quad (1)$$

where A_0 and A_1 are the initial asymmetries of the slow and fast relaxation components and λ_0 and λ_1 are the respective muon spin depolarization rates. $G_Z(\Delta, H_{LF}, t)$ is the static Kubo–Toyabe function.[7] Δ/γ_μ is the distribution width of the nuclear-dipole fields at the muon sites, and γ_μ is the gyromagnetic ratio of muon spin. The H_{LF} is the longitudinal field. In the case of zero-field, H_{LF} is set to zero. Figure 2 shows the time scale and the schematic representation of muon spectroscopy.

Figure 3 shows the initial asymmetries and the depolarization rates as a function of temperature from 1.9 to 40 K for n = 3 – 5.[8] As shown in Fig. 3(a), when the temperature decreases from 40 K to the Curie temperature, the initial asymmetry shows a remarkable drop and reaches about 1/3 of that at 40 K, then it remains unchanged below the Curie temperature. The remarkable drop in the initial asymmetry between 30 K and the Curie temperature is attributed to the

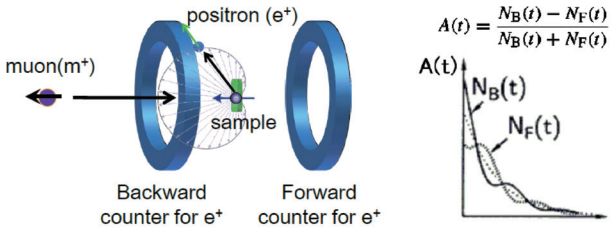

Figure 2. Time scale and the schematic representation of muon spectroscopy. $N_F(t)$ and $N_B(t)$ are the total muon events of the forward and backward counters aligned in the beam line, respectively.

development of 2D ferromagnetic short-range order, which is explained by the mechanism that the time scale of fast relaxation caused by the ferromagnetic ordering crosses the time window of μSR measurement. As shown in Fig. 3(b), the depolarization rate of the ZF-μSR exhibits an anomalous peak at around the inflection point in the drop of initial asymmetry as a function of temperature, which is due to the critical slowing down of the Fe spin fluctuation toward the ferromagnetic transition. In the case of n = 4, there is only one peak in the temperature dependence of the depolarization rate, while the ferromagnetic transition shows two peaks in the ZFCM. This inconsistency is caused by the difficulty to detect the muon spin depolarization rate of LTP, because the internal field of HTP accelerate the decay of spin-polarized muon which interacts with LTP ordering state.

In addition to the ferromagnetic transition for $(n\text{-}C_nH_{2n+1})_4N[Fe^{II}Fe^{III}(dto)_3]$ (n = 3 – 5), the CTPT was also detected by μSR in $(n\text{-}C_3H_7)_4N[Fe^{II}Fe^{III}(dto)_3]$. Figure 4 shows the time spectra of μSR for $(n\text{-}C_3H_7)_4N[Fe^{II}Fe^{III}(dto)_3]$ at several temperatures under zero-field.[2,4] In this figure, we can observe a difference between the time spectra of heating and

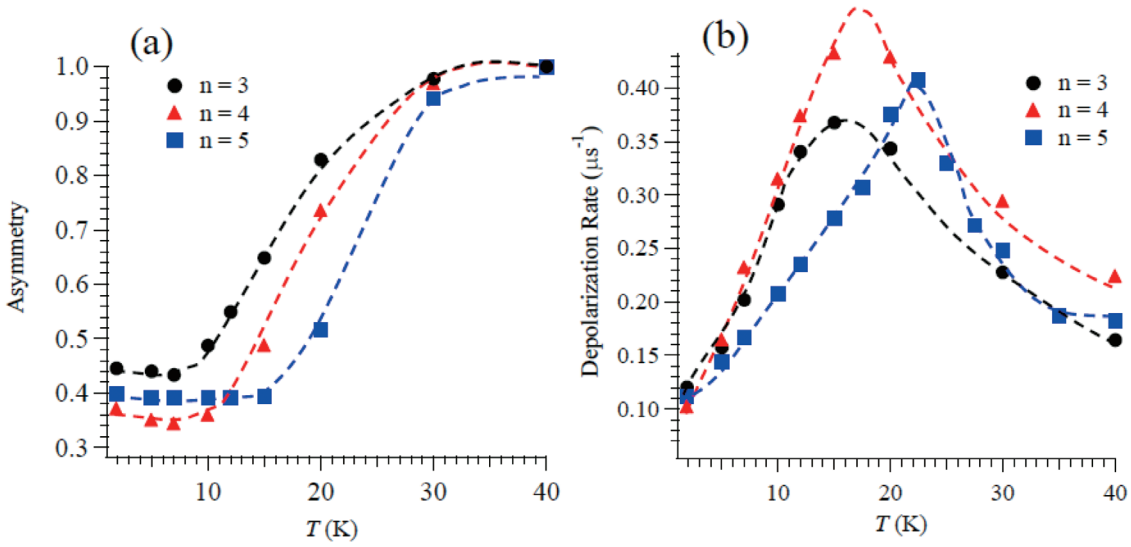

Figure 3. (a) Initial asymmetry and (b) depolarization rate as a function of temperature for $(n\text{-}C_nH_{2n+1})_4N[Fe^{II}Fe^{III}(dto)_3]$ (n = 3 – 5). Dashed lines are guides for eyes.

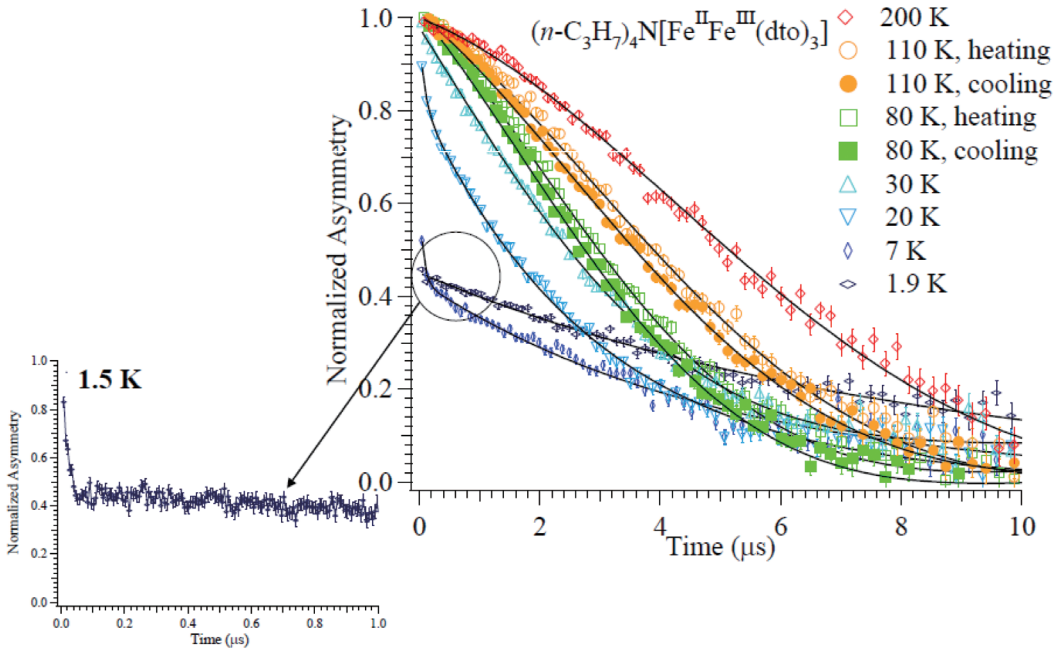

Figure 4. Time spectra of μSR for $(n\text{-}C_3H_7)_4N[Fe^{II}Fe^{III}(dto)_3]$ at several temperatures under zero-field. There are differences between the spectra under heating and cooling process only at 80 and 110 K.

cooling processes at 80 and 110 K, while no such difference is detected for the spectra above 200 K or below 30 K.

From the analysis of these spectra by using eq. (1), we can obtain the temperature dependence of the depolarization rate for $(n\text{-}C_3H_7)_4N[Fe^{II}Fe^{III}(dto)_3]$ (see Fig. 5). The same analysis as $n = 3$ can be applied to the time spectra for $n = 5$, and the corresponding data for $n = 5$ is shown in Fig. 5. These depolarization rates as a function of temperature show the peaks at 15 and 22 K for $n = 3$ and 5, respectively, due to the critical slowing down of the fluctuations of Fe spins toward the ferromagnetic transition.[9] Moreover, in the case of $n = 3$, an anomalous enhancement of depolarization rate with thermal hysteresis between 60 and 140 K appears, while $n = 5$ shows no such anomaly. The temperature range where the anomalous enhancement of depolarization rate appears corresponds to the hysteresis loop of the CTPT for $n = 3$. Therefore, the anomalous enhancement of depolarization rate with thermal hysteresis around 80 K for $n = 3$ obviously originates from the CTPT. Taking into account that the CTPT is accompanied by the electron transfer and the HTP state is mixed with the LTP state around 80 K, it is concluded that the electron transfer between the Fe^{II} and Fe^{III} sites induces the fluctuating internal fields at the muon site, which enhances the depolarization rate. Therefore, the oscillation of electrons between the Fe^{II} and Fe^{III} sites is responsible for the dynamical nature of the CTPT.

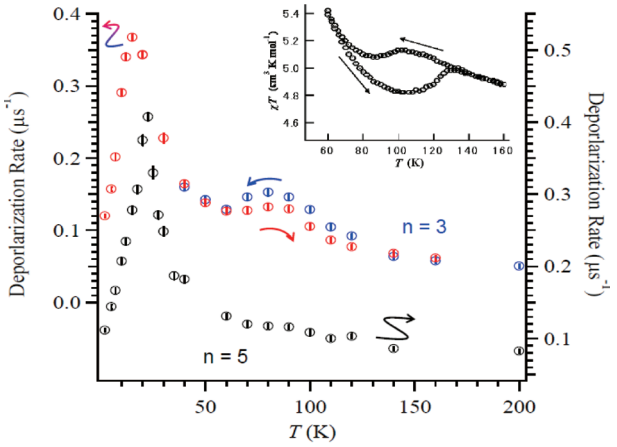

Figure 5. Temperature dependence of the dynamic muon spin depolarization rate, λ_0, for $(n\text{-}C_3H_7)_4N[Fe^{II}Fe^{III}(dto)_3]$ in cooling and heating processes and $(n\text{-}C_5H_{11})_4N[Fe^{II}Fe^{III}(dto)_3]$. The inset shows the temperature dependence of molar magnetic susceptibility multiplied by temperature for $(n\text{-}C_3H_7)_4N[Fe^{II}Fe^{III}(dto)_3]$. Arrows denote the direction of the temperature change.

Figure 6 shows the depolarization rate of muon spin as a function of temperature under various longitudinal magnetic field. In the case of $n = 3$, the anomalous peak around 80 K attributed to the CTPT decreases and disappears with increasing the longitudinal field. In the case of $n = 5$, on the other hand, no peak is observed between 200 and 40 K.

As shown in Fig. 6, the depolarization rates for both complexes decrease with increasing longitudinal field up to about 100 Oe and become constant above that field. The constant values increase with decreasing temperature. This behavior suggests the existence of two components. One component is easily suppressed by the weak longitudinal field

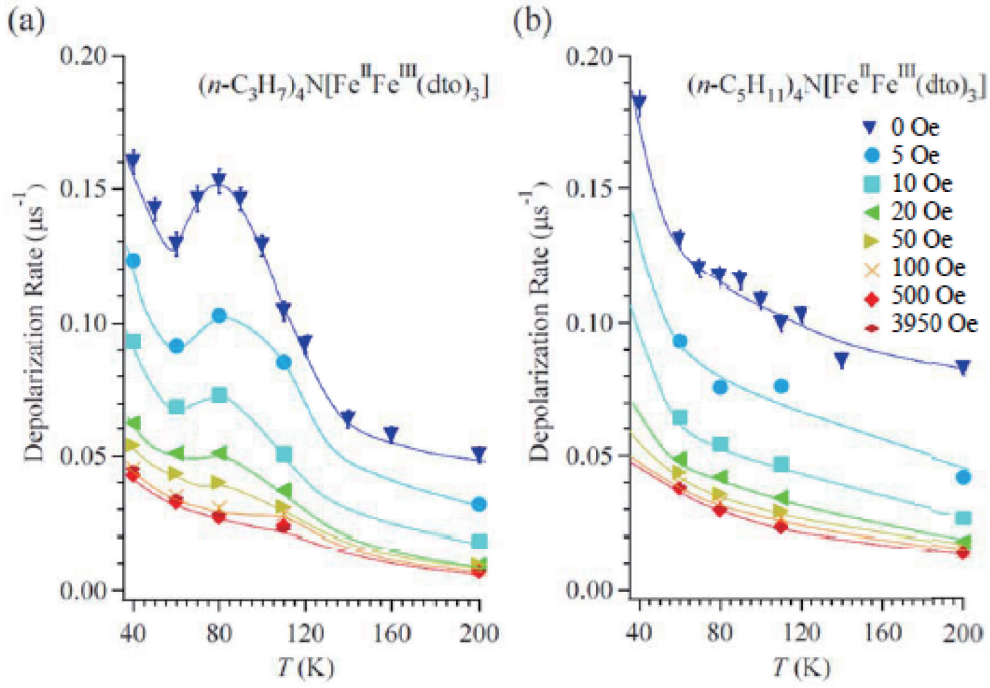

Figure 6. (a) Temperature and longitudinal-field dependence of the dynamic muon spin depolarization rate, λ_0, for $(n\text{-}C_3H_7)_4N[Fe^{II}Fe^{III}(dto)_3]$. (b) Temperature and longitudinal-field dependence of λ_0 for $(n\text{-}C_5H_{11})_4N[Fe^{II}Fe^{III}(dto)_3]$. The solid lines are guides for the eye.

of 100 Oe, and the other one remains under the longitudinal field up to 4 kOe. The former component implies that there is a weak and slowly fluctuating internal field at the muon site, which is easily masked by the weak longitudinal field of 100 Oe. The origin of the former component is due to the fluctuating component of nuclear dipoles as has been observed in MnSi.[10] On the other hand, considering that the latter component increases with decreasing temperature and similar values of the depolarization rate are observed in both cases of n = 3 and 5 at the same temperature, it is suggested that the latter component originates from the dipole field of dynamically fluctuating Fe spins.

Turning to the anomalous enhancement of the depolarization rate of muon spin due to the CTPT, we extract the difference of depolarization rate between those of n = 3 and 5 to analyze the fluctuation of electrons between the Fe^{II} and Fe^{III} sites at the CTPT. The field dependence of this subtracted depolarization rate at 80 K is plotted in Fig. 7. Applying the Redfield's equation[11–13] to the longitudinal field (H_{LF}) dependence of the subtracted depolarization rate (λ_{CT}) between n = 3 and 5, we can evaluate the correlation time of muon spins (τ_c) and the amplitude of the fluctuating internal field (H_{loc}) at the muon site, respectively. The formula of this equation is expressed as follows,

$$\lambda_{CT} = \frac{2\gamma_\mu^2 H_{loc}^2 \tau_C}{1 + \gamma_\mu^2 H_{LF}^2 \tau_C^2} \qquad (2)$$

where γ_μ is the gyromagnetic ratio of muon spin. These parameters at several temperatures are summarized in Table 1.

Table 1. Parameters obtained by fitting with Redfield equation to the subtracted depolarization rate.

T (K)	τ_C (μs)	H_{loc} (G)
60	——	0
80	5.7	4.0
110	10.6	1.9

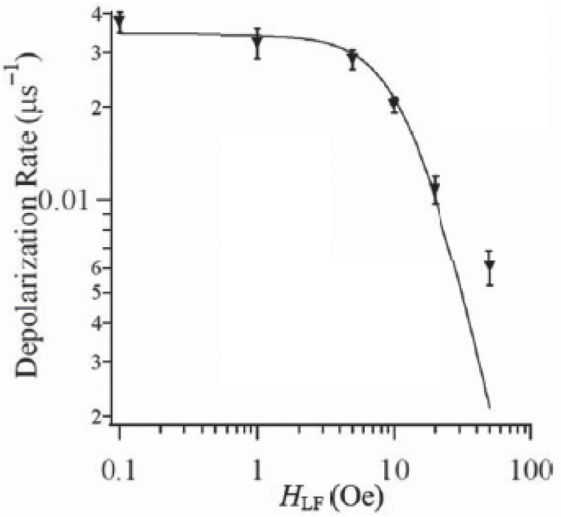

Figure 7. Longitudinal-field dependence of the dynamic muon spin depolarization rate, λ_{CT}, corresponding to the charge transfer phase transition for $(n\text{-}C_3H_7)_4N[Fe^{II}Fe^{III}(dto)_3]$ at 80 K in the cooling process.[2,4] The solid line shows the best fit of eq. (2).

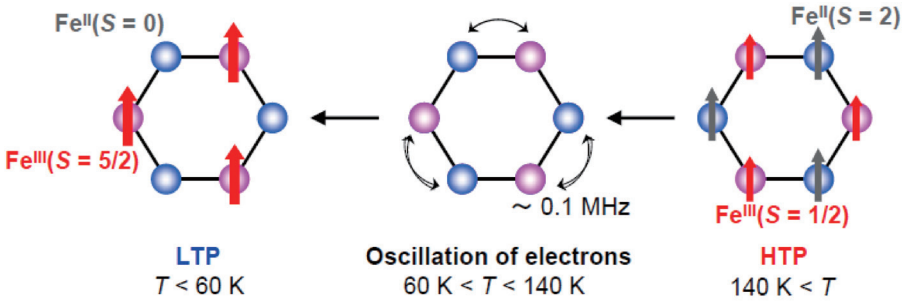

Figure 8. Schematic representation of the valence fluctuation between the Fe^{II} and Fe^{III} sites at the charge transfer phase transition (CTPT) for $(n\text{-}C_3H_7)_4N[Fe^{II}Fe^{III}(dto)_3]$.

The frequency of the additional internal field at the muon site, which is given as $\nu = 1/\tau_c$, is the order of 0.1 MHz as the maximum at 80 K and zero at 60 K.[2,4] The magnitude of H_{loc} is between 1.9 and 4.0 G, which is larger than that of nuclear dipole field (~1 G). These results of μSR measurement suggest the existence of dynamic electron fluctuation between Fe^{II} and Fe^{III} sites with its frequency of 0.1 MHz at 80 K, which is schematically shown in Fig. 8. The time scale of τ_c is consistent with the result of the ^{57}Fe Mössbauer measurement which implies that the fluctuation between the HTP and LTP is slower than 10^{-7} s.[4] Considering the dynamic electron fluctuation between the Fe^{II} and Fe^{III} sites in $[Fe^{II}Fe^{III}(dto)_3]$ layer, the electron hopping conduction is induced by the CTPT. This behavior is consistent with the anomalous drop with thermal hysteresis in the electrical resistivity at the CTPT.[4] Considering that the CTPT in this system is the first order phase transition, the dynamically fluctuated valence state of iron is regarded as the fluctuation of chemical potential between the high-temperature phase (HTP) and the low-temperature one (LTP).

5. DIELECTRIC RESPONSE AT THE CTPT

Dielectric constant measurement is one of the most powerful methods to investigate dielectric materials. Recently, charge order driven ferroelectrics have been developed to realize a large dielectric constant, fast response to polarization inversion and high density of polarization domains.[14] Moreover, dielectric constant measurement is also useful for the investigation of characteristic properties of charge-transfer or proton-transfer molecular materials. For example, neutral-ionic transition between donor and accepter molecules is responsible for the large dielectric response.[15] These results suggest that the dielectric constant measurement is valuable for its application to electron transfer phenomena. In the case of $(n\text{-}C_3H_7)_4N[Fe^{II}Fe^{III}(dto)_3]$, it is expected that an anomalous enhancement of the dielectric constant is associated with the CTPT.

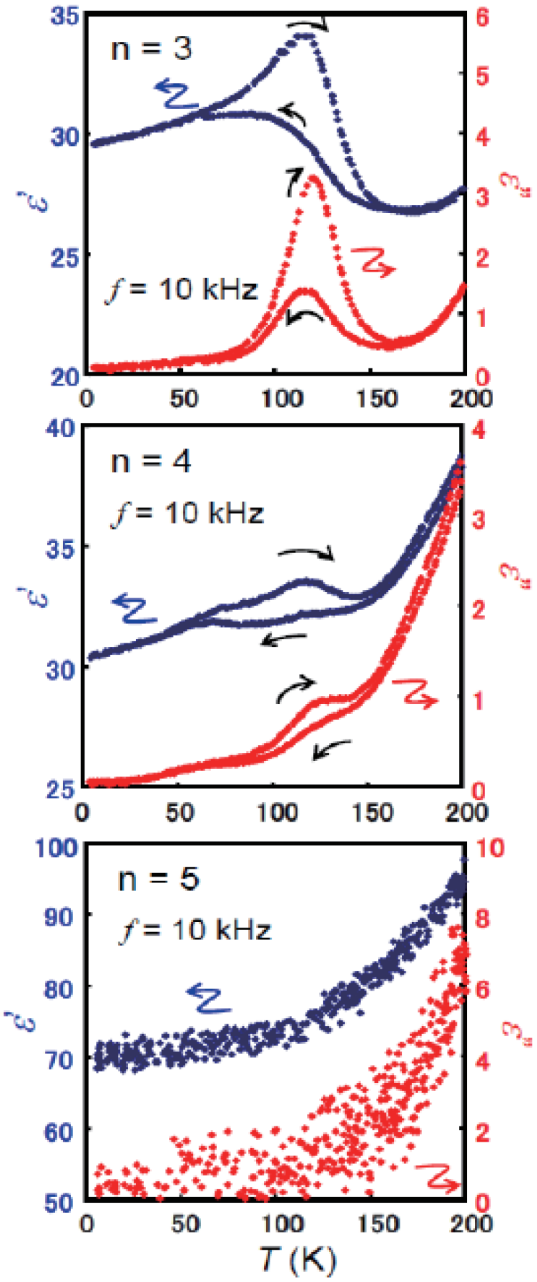

Figure 9. Temperature dependence of the in-phase (upper) and the out of phase (lower) parts of the dielectric constant with the frequency of 10 kHz for $(n\text{-}C_nH_{2n+1})_4N[Fe^{II}Fe^{III}(dto)_3]$ (n = 3 – 5).

From the viewpoint of the characteristics of dielectric constant, we measured the temperature dependence of the dielectric constant to directly observe the CTPT in $(n\text{-}C_nH_{2n+1})_4N[Fe^{II}Fe^{III}(dto)_3]$ (n = 3 – 5). As shown in Fig. 9, anomalous enhancements in the real and imaginary components of dielectric constants for n = 3 and 4 were observed in the same temperature range of CTPT, while no anomaly was observed for n = 5. The increments of ε' and ε'' above 150 K are attributed to the dynamical motion of $(n\text{-}C_nH_{2n+1})_4N^+$. The temperature range of the hysteresis loop is independent of the applied frequency. Judging from the results of μSR and dielectric constant measurements, the anomalous enhancement of dielectric constant is attributed to the dynamical fluctuation of electrons between the Fe^{II} and Fe^{III} sites. As shown in Fig. 10, the anomalous enhancement of the dielectric constant induced by the CTPT remarkably depends on the frequency of electric field and it becomes apparent as the frequency of electric field is lowered to 1 Hz, which is quite similar to the dielectric relaxation in relaxor ferroelectrics. Such frequency dependence is considered to be caused by the slow relaxation of the electrons, due to the barrier of the electron hopping on the grain boundary of domains.

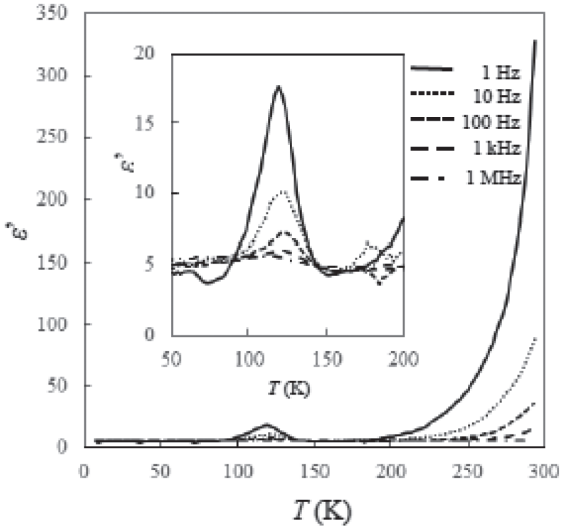

Figure 10. Temperature- and frequency-dependent dielectric constant under heating process for $(n\text{-}C_3H_7)_4N[Fe^{II}Fe^{III}(dto)_3]$. Inset shows the magnified view in the vicinity of the CTPT.

6. CONCLUSION

We have developed a ferromagnetic organic-inorganic hybrid system, $A[Fe^{II}Fe^{III}(dto)_3]$ (A = $(n\text{-}C_nH_{2n+1})_4N$, spiropyran, etc.), and discovered the charge transfer phase transition (CTPT) for $(n\text{-}C_nH_{2n+1})_4NFe^{II}Fe^{III}(dto)_3]$ (n = 3 and 4), where the thermally induced charge transfer between the Fe^{II} and Fe^{III} sites occurs reversibly. In order to detect the dynamic process of CTPT, we carried out the μSR and dielectric constant measurement techniques for these complexes. From the analysis of μSR, we revealed the dynamics of CTPT for $(n\text{-}C_3H_7)_4N[Fe^{II}Fe^{III}(dto)_3]$. In particular, it is notable that the hopping rate of electrons between the Fe^{II} and Fe^{III} sites at the CTPT is evaluated at 0.1 MHz by the analysis of the μSR under longitudinal magnetic field. On the other hand, the dielectric constant measurement is very sensitive for detecting the existence of CTPT. In the cases of $(n\text{-}C_nH_{2n+1})_4N[Fe^{II}Fe^{III}(dto)_3]$, an anomalous enhancement of dielectric constant with thermal hysteresis appears at the CTPT across the whole measuring frequency range between 1 Hz and 1 MHz, which is attributed to the valence fluctuation between Fe^{II} and Fe^{III} sites associated with the CTPT. This anomaly becomes enhanced as the frequency is lowered, which is quite similar to the dielectric relaxation in relaxor ferroelectrics. Considering that the CTPT in this system is the first order phase transition, the dynamically fluctuated valence state of iron is regarded as the fluctuation of chemical potential between the high-temperature phase and the low-temperature one.

ACKNOWLEDGMENT

This research has been supported by the following collaborators, Dr. Masaya Enomoto (Tokyo University of Science), Dr. Isao Watanabe (RIKEN), Prof. Miho Itoi (Nihon University School of Medicine), Dr. Noriyuki Kida (Mitsubishi Chemical Co.). The author wishes to thank the collaborators for the muon spectroscopy and dielectric constant measurements.

REFERENCES

1) ***a)*** N. Kojima, W. Aoki, M. Itoi, Y. Ono, M. Seto, Y. Kobayashi, Yu. Maeda, *Solid State Commun*., **120** (2001) 165, ***b)*** T. Nakamoto, Y. Miyazaki, M. Itoi, Y. Ono, N. Kojima, M. Sorai, *Angew. Chem.Int. Ed*., **40** (2001) 4716, ***c)*** M. Itoi, Y. Ono, N. Kojima, K. Kato, K. Osaka, M. Takata, *Eur. J. Inorg. Chem*., **2006** (2006) 1198.
2) N. Kida, M. Enomoto, I. Watanabe, T. Suzuki, N. Kojima, *Phys. Rev. B* **77** (2008) 144427-1.
3) N. Kojima, M. Itoi, Y. Miyazaki, *Current Inorg. Chem*., **4** (2014) 85.
4) M. Enomoto, I. Watanabe, N. Kojima, *Current Inorg. Chem*., **6** (2016) 49.
5) M. Itoi, A. Taira, M. Enomoto, N. Matsushita, N. Kojima, Y. Kobayashi, K. Asai, K. Koyama, T. Nakano, Y. Uwatoko, J. Yamaura, *Solid State Commun*., **130** (2004) 415.
6) I. Watanabe, Y. Ishii, T. Kawamata, T. Suzuki, F. L. Pratt, R. Done, M. Chowdhury, C. Goodway, J. Dreyer, C. Smith, M. Southern, *Physica B: Condensed Matter*, **404** (2009) 993.

7) R. S. Hayano, Y. J. Uemura, J. Imazato, N. Nishida, T. Yamazaki, R. Kubo, *Phys. Rev. B* **20** (1979) 850.
8) M. Enomoto, N. Kida, I. Watanabe, T. Suzuki, N. Kojima, *Physica B: Condensed Matter*, **404** (2009) 642.
9) O. Hartmann, *Hyperfine Interact.*, **49** (1989) 61, and references cited therein.
10) R. Kadono, T. Matsuzaki, T. Yamazaki, S. R. Kreitzman, J. H. Brewer, *Phys. Rev. B* **42** (1990) 6515.
11) L. P. Le, A. Keren, M. I. Larkin, G. M. Luke, W. D. Wu, Y. J. Uemura, J. S. Miller, A. J. Epstein, *Phys. Rev. B* **65** (2001) 024432-1.
12) W. Higemoto, H. Tanaka, I. Watanabe, K. Nagamine, *Phys. Lett. A* **243** (1998) 80.
13) C. P. Slichter, Principles of Magnetic Resonance, Springer-Verlag, Berlin, Heidelberg, 1978.
14) S-W. Cheong, M. Mostovoy, *Nature materials*, **6** (2007) 13.
15) K. Kobayashi, S. Horiuchi, R. Kumai, F. Kagawa, Y. Murakami, Y. Tokura, *Phys. Rev. Lett.*, **108** (2012) 237601-1.